19810 pgs pgs

INSTITUTE OF COAL RESEARCH
The University of Newcastle

JOINT COAL BOARD—INSTITUTE OF COAL RESEARCH

RESEARCH PROJECT

'IDENTIFICATION OF FABRIC DEFECTS LEADING TO ROOF FAILURE UNDER MINING INDUCED LOADING'

PROGRESS REPORT ON MECHANICAL TESTS PERFORMED IN THE PERIOD FROM JULY 1994 TO FEBRUARY 1995

by
G. LI
and
K.H.R. MOELLE

March 1995

INDEX

I. EXECUTIVE SUMMARY

The second report on progress of the JCB–sponsored ICR research project on 'Relationship Between Rock Fabric Defects and Sudden Uncontrolled Roof Failures in NSW Collieries' and 'Identification of Fabric Defects Leading to Roof Failure Under Mining Induced Loading' contains the results of tests made on rocks from 9 collieries and 2 other mining sites.

The work done over the past six months brings an important phase of the research project to a conclusion. That phase has established the foundations of a data base and identified the appropriate test methods and techniques for specimens from coal measures rocks.

The next phase will concentrate on the specific testing of rocks with geological defects and also of rocks obtained from areas in collieries where roof failures have occurred over the past two years.

The role of defects in the mechanical response of coal measures rocks to directed loading has been studied in considerable detail.

A new technique has been developed to allow the preparation of suitable test specimens from highly anisotropic and mechanically weak samples.

Two existing test methods for the establishment of fracture toughness (K_{IC}) values have been critically examined in the course of the investigations and found to be inadequate for the testing of some coal measures rocks. A suitable method has now been developed by the ICR.

Stable fracture development commences in many of the tested sandstones much earlier than in most other rocks. This is a very important finding and result relevant to the design of rock- and fracture mechanics investigations and to the interpretation of results.

II. INTRODUCTION

This is the ICR's second progress report on mechanical testing of coal measures rocks since the installation of the MTS 318.50 closed-loop electro-hydraulic testing facility in December 1993. The testing device, purchased with a grant from the JCB Health and Safety Trust Fund, is used to study the mechanical performance of coal and coal measures rocks under directed load. Particular emphasis has been put on the brittle deformation (fracture) response of the tested rocks, in an attempt to study the effects of fabric defects on sudden roof failures experienced in NSW underground coal mines in order to identify the nature of links between roof failures and certain fabric configurations. Such links need to be identified to improve strata control practices, especially as no other research institution currently investigates the role of rock fabric configurations and defects in the processes leading to loss of cohesion or mechanical disintegration of roofstrata.

The first progress report to the Joint Coal Board was prepared by the Institute of Coal Research (ICR) in July 1994, it summarised mechanical test data obtained from specimens collected during an extended sampling programme at Muswellbrook No. 2 Colliery. The test programme has since been significantly expanded, and to date a wide range of rock types has been tested, comprising samples from several collieries in the Southern Coalfield as well as in the Hunter Valley. A small number of samples from Queensland collieries has also been tested. The testing of laminite specimens, a rock type responsible for considerable difficulties in strata control, has been prioritised and studied in considerable detail.

The present phase of the research programme will conclude with the development of a computerised data base of test results obtained with the MTS load frame. Such a data base will enable correlations among the recorded failure incidents, the structural and sedimentological attributes of the tested rocks, and the mechanical test data. Statistical analyses and cross-correlations should then provide useful information for the identification of relevant attributes that will conceivably lead to the prediction of sudden uncontrolled failures. This report summarises the test data gathered since the installation of the MTS testing device, and discusses mechanical and fracture patterns observed on the rocks tested.

Sample preparation techniques have been developed over the past six months by the ICR and three existing preparation methods have been critically assessed.

III. EXPERIMENTAL PROGRAMME

The three major types of tests, UCS (Uniaxial Compressive Strength Tests), Brazil Tensile Strength Tests, and Fracture Toughness Tests (K_{IC}) , continue to provide the basis for the experimental test and research programme, which aims at the characterisation of the mechanical and fracture behaviour patterns of rock samples collected from NSW collieries. The samples have been collected from roof- and floor strata of coal seams, from the overburden sequence, as well as from some igneous intrusive rocks to cover the physical properties of the full range of rocks likely to be encountered during underground mining operations.

Bed separation in laminated rocks has traditionally been one of the primary causes for roof failures in Australian underground mines. It is important to understand the fracture and failure mechanisms of these rocks during fracturing processes along bedding planes. A specific experimental programme has been included in the present investigation that involves the assessment of the influence of 'laminae' bedding in those rocks on fracture initiation and propagation. Test core specimens have been drilled from large samples parallel and normal to the laminae.

IV. DEVELOPMENT OF DATA BASES FOR THE MANAGEMENT OF TEST RESULTS

The installation of the MTS testing device has allowed the development of an increasingly large data base for the mechanical properties of coal and coal measures rocks from NSW collieries. It has laid the foundations for a comprehensive understanding of the mechanical behaviour patterns of the roofstrata in several collieries, with a view to improving strata control. The information gathered by the present test programme will be statistically analysed, and the mechanical attributes of the tested rocks will be correlated with their structural and sedimentological attributes to categorise the performance patterns of the 'roof–seam–floor' system of the areas studied.

Appendix A of this report is a catalogue of the data produced with the MTS testing machine, including 138 compressive strength tests, 116 tensile strength tests and 90 fracture toughness tests. Apart from the data listed in Appendix A, the deformation or fracture process observed during each of the tests has been electronically recorded for subsequent detailed analyses.

V. DEVELOPMENT OF TESTING TECHNIQUES

STUDYING FRACTURE DEVELOPMENT IN LAMINATED SOFT ROCKS

Studies on fracture propagation patterns along the laminae of laminated soft rocks are an important aspect for the understanding and prevention of sudden uncontrolled roof failures in underground coal mines. The current investigation attempted initially to use the ISRM standard fracture testing method [1] as a test procedure, however it was soon found that the 'standard method' was not suitable for anisotropic and weak laminites found in the coal measures sequences.

A new testing method, specifically designed for fracture toughness testing of these rocks, has been developed. The new procedure is based on a disk-shaped test specimen geometry; the disk is subjected to diametral compression during the test. The method has several advantages over that prescribed by the ISRM [1].

- The disk-shaped test specimens can be readily prepared from laminated soft rocks that tend to disintegrate into disks during preparation and testing. The specimen geometry required for the ISRM method is totally unsuitable for these rocks.

- More than 90% of the test specimens prepared from soft laminated rocks and coal samples according to the ISRM method, failed prematurely in tests; in many cases even the specimen preparation was unsuccessful. In contrast, testing of disk-shaped specimens has been successful in most instances.

- The new testing methods allow the evaluation of structural anisotropies and their influence by using a single type of specimen geometry. This cannot be achieved by testing of specimens prepared according to the ISRM method.

Two previously developed disk testing techniques [2, 3] have been assessed during the past six months in the course of routine tests, and a special experimental programme was instituted to check their validity. Cores of various geological materials, mainly sandstones, were selected for these checks. The selected cores were of sufficient length and displayed statistical uniformity in fabric and composition over their total length. Short Rod specimens [1], two disk specimens cut according to Szendi-Horvath [2], and Guo *et al* [3], respectively, were then prepared from the same core, forming a data group (Fig. 1). Fracture toughness values obtained from tests conducted according to the three different testing methods on the same core were then compared. The fracture toughness value derived from the standard Short Rod specimen was regarded as the correct value.

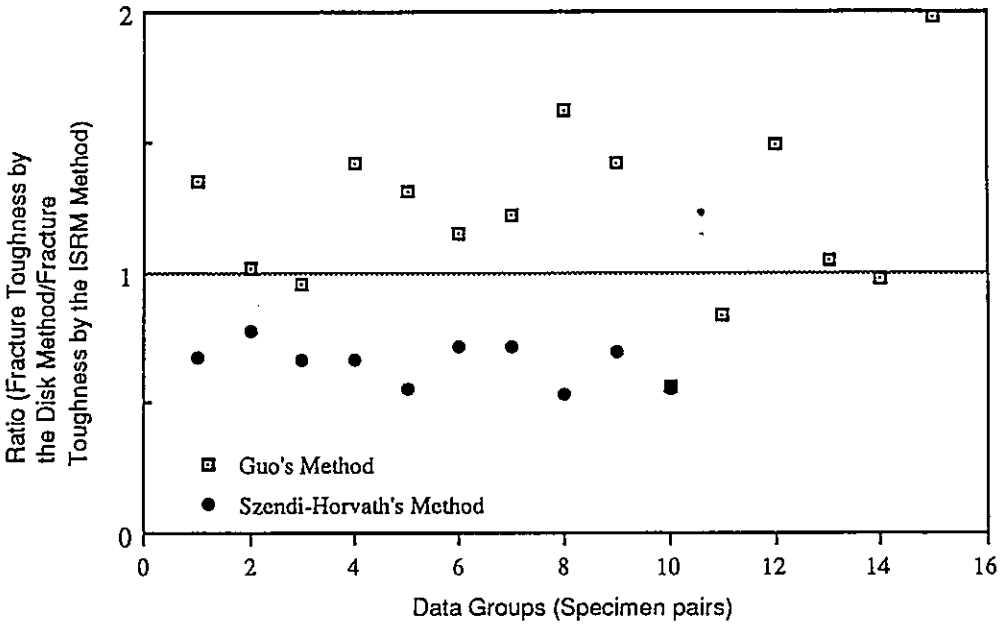

Fig. 1. The ratio of $K_{IC.Disk}$ values to $K_{IC.Stand}$ values.

Figure 1 illustrates the ratio of fracture toughness values obtained by the two disk methods to those achieved by the ISRM method. Guo's method tends to overestimate the fracture toughness of the tested rocks, whereas the Szendi-Horvath's method produces the opposite effect (Fig. 1). Severe scatter is found among fracture toughness values derived from Guo's method, compared with that resulting from the application of Szendi-Horvath's method (Fig. 1).

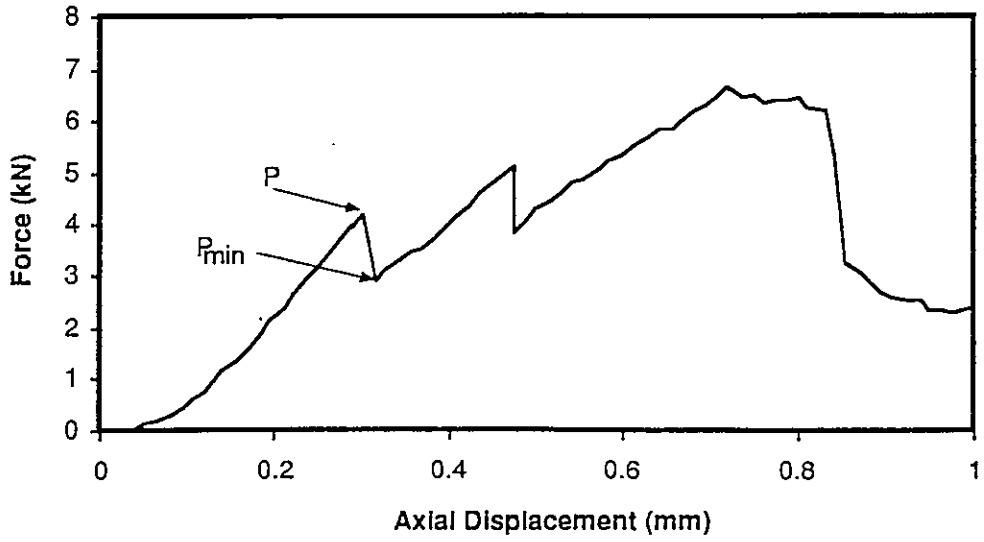

Fig. 2. A typical Brazil test record, showing the local minimum load P_{min} and the fracture inducing load P.

The testing method proposed by Guo *et al* [3] is based on the concept of the Brazil test procedure, but it uses the minimum load P_{min}, as shown in Fig. 2, to calculate fracture toughness. The present authors consider that the use of P_{min} is inappropriate, since the energy stored in the test system (load frame) during a test can significantly affect the value of P_{min}, depending on the type of test equipment used and on the materials tested. Consequently, the derived fracture toughness does not accurately reflect that mechanical property of the material. This is regarded as a serious flaw in the testing method developed by Guo *et al* [3], as it overestimates the fracture resistance of the tested material.

Due to the significant difference between the fracture toughness values obtained by the two proposed disk methods, and those by the ISRM method (Fig. 1), the ICR is presently developing a new testing method based on the 'Chevron Notched Disk Specimen' geometry. Theoretically, that testing method is similar to the ISRM standard testing method [1], but has been modified specifically to suit highly anisotropic and mechanically weak rocks.

IDENTIFICATION OF ONSET OF UNSTABLE FRACTURING

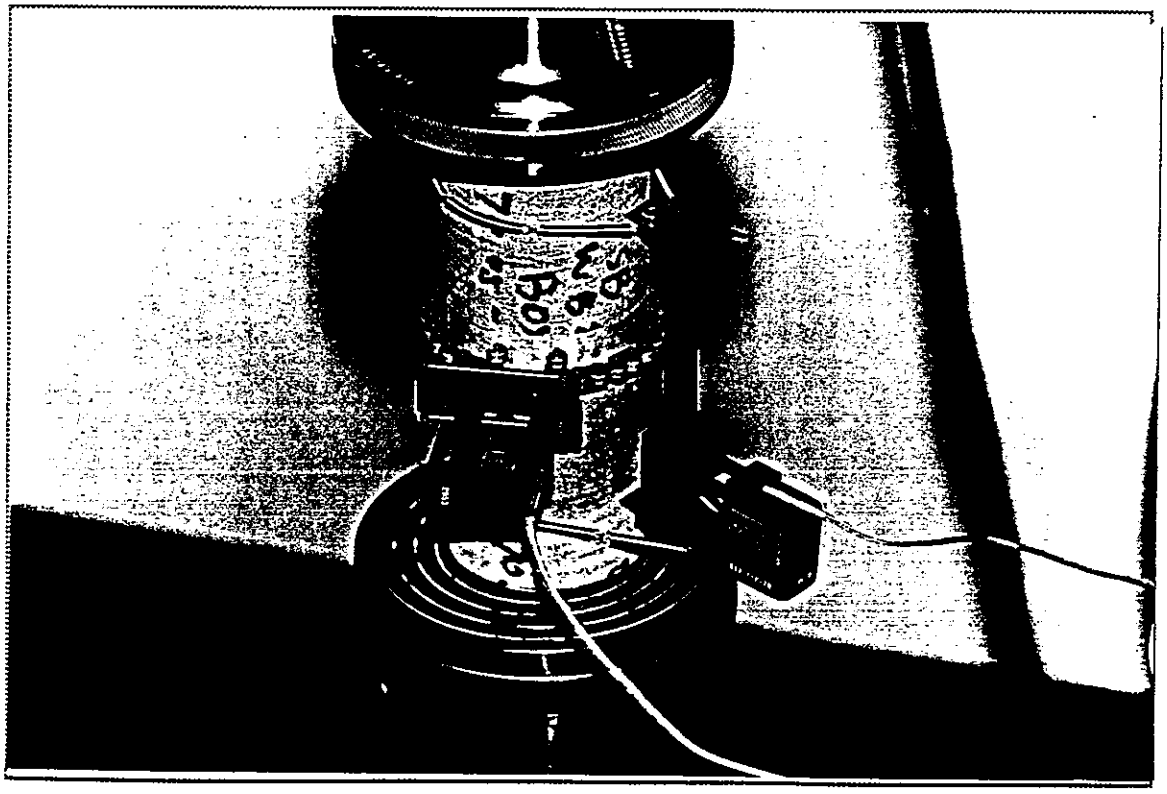

Fig. 3 The experimental set-up for a uniaxial compressive strength test with the equipment for axial and circumferential strain measurements attached to the core specimen.

Figure 3 shows a cylindrical specimen tested under uniaxial compressive load condition, with the recently installed MTS axial and circumferential strain extensometers. Volumetric strains are computed from the measured axial and circumferential strain data after the completion of the test. The stress-volumetric strain relationship identifies the fracture development in the tested specimens. The creation of fracture space in the specimens causes an increase in the specimen volume, a process called 'fracture dilation,' that is recorded as a negative volumetric strain element, and offset against the continuing compression of the specimen, a positive volumetric strain element.

Some selected sandstone specimens have been subjected to tests as shown in Fig. 3, to study their stress-strain relationships under load.

Figure 4 illustrates the typical stress-strain relationships of a rock specimen subjected to a uniaxial compressive load. Four distinct regions are highlighted in this diagram to allow a comparison between the characteristic patterns and the obtained stress-strain plots of sandstone specimens.

Region A: The non-linear portion of stress-strain curves, clearly portrayed by the stress-axial strain curve, indicates the closure of pores and pre-existing cracks oriented at 'favourable' angles to the applied load.

Region B: The stress-strain curves exhibit linearity, indicative of the occurrence of elastic deformation in this region.

Region C: This region is characterised by stable fracture development in the specimen, as manifested by the departure from linearity of the stress-volumetric strain curves (this does not usually apply to the stress-axial strain curve). Departure from linearity occurs at stress levels of approximately one-third to two-thirds of the UCS value for many rocks. Test results of coal measures rocks demonstrate stable fracture development at lower stress levels, and the mechanical peculiarity of coal measures rocks is again demonstrated. This finding has most important implications for all mechanical investigations on rocks in the producing coalfields.

Region D: In this region, unstable fracture development prevails and fractures propagate until the specimen loses cohesion and fails under stress. The inflection point on the stress-volumetric strain curve defines the onset of unstable fracturing.

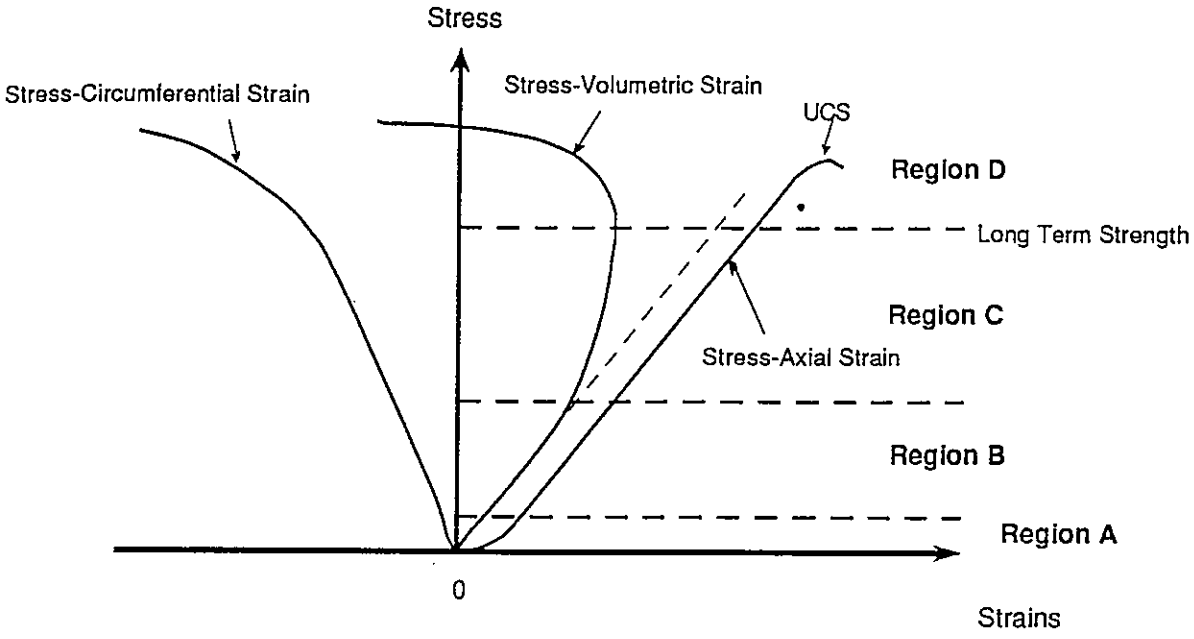

Fig. 4. Typical stress-strain relationships of a rock specimen subjected to uniaxial compressive load in an unconfined configuration.

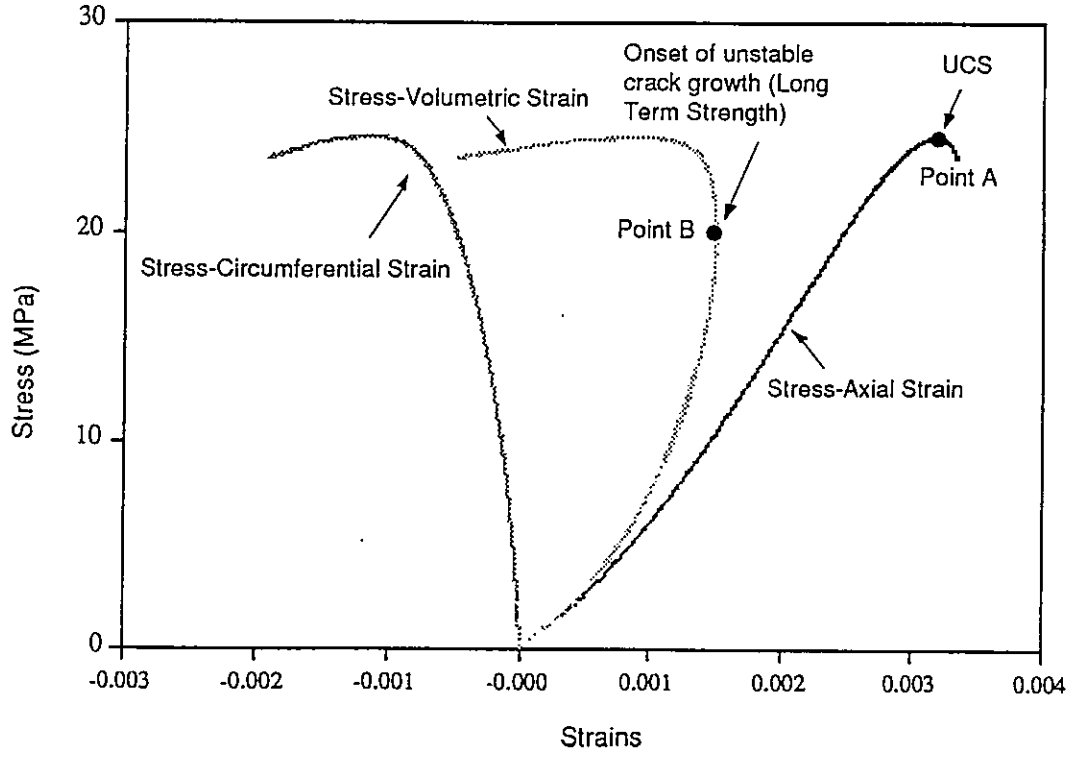

Fig. 5. Characteristic stress-strain relationships found in a tested sandstone specimen depicting the axial, circumferential and volumetric strains, respectively.

In contrast to the stress-volumetric strain curve shown in Fig. 4, and found in most rocks, the stress-volumetric strain curves of the sandstone specimens tested are non-linear. This indicates that test-induced fracturing commenced in the specimens at a very low stress level, generally at only 18% of the specimens' ultimate strength values (Fig. 5). The initiation of such fractures and their development is a very important sequence in the eventual failure process of the rocks tested. More work is required to identify the critical stages of fracture initiation and propagation in the fabric of the rock under load. The use of acoustic emission detection instruments will later assist in the analytical assessments of these phenomena.

At a stress level of approximately 80% of the specimens' strength values, unstable fracturing in the tested specimens starts to develop, as portrayed by the inflection point on the stress-volumetric strain curves. The development of unstable fracturing will eventually lead to specimen failure over time, provided that the stress level is greater than 80% of the specimens' UCS values.

The inflection point on the stress-volumetric strain curve signifies an important change in the deformation process of a specimen tested under uniaxial compressive loading conditions. Up to this point, compression of a specimen's volume is the primary deformation process, whereas beyond it, unstable fracturing will dominate.

Studies by the ICR on unstable fracturing will be extended to other coal-measures rock types with different defect configurations. The future study and research will also be combined with the use of acoustic emission sensors, to identify and categorise any early warning signals for imminent failures that may have common patterns.

VI. MECHANICAL RESPONSE OF HIGHLY ANISOTROPIC COAL MEASURES ROCKS TO DIRECTED LOADING

Conventional underground and, more recently, also highwall operations, suffer from roof instability caused by bed separation and disintegration of laminites in the immediate roofstrata. Laminites are sedimentary rocks consisting of laminae (maximum thickness 10 mm), and made up of sandstone, siltstone, mudstone, claystone, carbargillite and coal. The mechanical response of laminites to the application of stresses is governed almost exclusively by their petrological composition, micro-texture and configuration of their fabric components. Several laminite fabric patterns depict preferred orientation in the form of imbrication structures and statistically preferred alignments of components according to their longest dimension. Such anisotropic fabric arrangements may also constitute strength anisotropies. Laminites with an abundance of clay minerals and/or zeolites usually fail rapidly, while the presence of calcite or quartz on the surface of laminae will delay failure, occasionally quite considerably.

INFLUENCE OF FABRIC ANISOTROPY AND PETROLOGICAL COMPOSITION

To evaluate the influence and effects of fabric anisotropy and petrological composition on the rock's stability, different rock types, including sandstone, siltstone, claystone and shale, were tested in this programme. All tested rocks displayed a high degree of structural anisotropy.

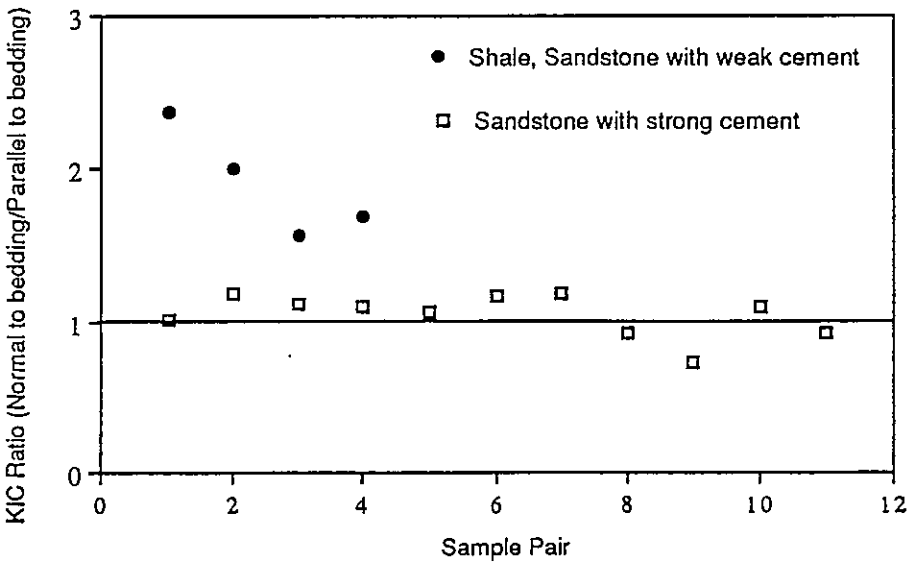

Fig. 6. The ratio of fracture toughness (K_{IC}) normal to bedding to that parallel to bedding.

The testing programme consisted of fracture toughness and UCS tests. Cores of sufficient length and statistical homogeneity were used to prepare pairs of specimens for fracture toughness or UCS tests. One specimen of the pair was tested with the fracture propagating (or loading direction in the case of UCS tests) normal to bedding, whereas the other specimen was loaded parallel to bedding. The difference in fracture toughness or UCS values between the two paired specimens would thus reflect the influence of the principal structural anisotropy. The difference in fracture toughness values between the paired specimens is shown in Fig. 6, depicting the ratio of the fracture toughness values obtained by loading normal and parallel to bedding.

A similar pattern as shown in Fig. 6 has also been observed for the UCS values obtained from the paired specimens.

The following observations have been made during the experimental test programme with paired specimens:

(i) Sandstone specimens with strong siliceous and/or carbonate cement did not show noticeable differences in fracture toughness or UCS values between the paired specimens (Fig. 6), although these specimens are structurally anisotropic.

(ii) In contrast, the fabric anisotropy in the sandstone specimens with high amounts of argillaceous cement and many chemically altered detrital clastic grains, has a strong influence on their fracture behaviour. The specimens' fracture resistance and UCS values are greater in the direction normal to bedding.

(iii) Shales and siltstones with clay minerals on the surfaces of well developed laminae, are strongly strength anisotropic. The fracture resistance for specimens with fracturing normal to bedding was approximately 2.0 to 2.5 times greater than that of specimens that developed fracturing parallel to bedding (Fig. 6). As discussed above, the ISRM method can only be used for relatively strong rocks. The fracture resistance or UCS of the majority of laminated weak rocks is considerably greater when tested normal to bedding rather than parallel to it. In this context it is also important to consider the difference between rock- and rockmass moduli and its influence on test results.

The above observations demonstrate that any assessment or modelling of the strength anisotropy of structurally 'defect' rocks must consider the petrological composition of the rocks under investigation. Not all structurally anisotropic rocks demonstrate also a strength anisotropy. However, laminites with an abundance of clay minerals are mechanically highly anisotropic, and may pose considerable difficulties for effective strata control. The significant strength anisotropy of the laminated and weak rocks will be further discussed in the following sections.

INFLUENCE OF STRUCTURAL DEFECTS ON FAILURE PROCESSES

In its last progress report, the ICR stated that the prediction and prevention of sudden uncontrolled failures of rocks in roofstrata requires a thorough understanding of fracture processes in coal measure rocks, and that fracture behaviour and the rapidity of rock failures are significantly affected by the fracture geometry created during the failure of the rocks.

A fracture system with a 'simple' geometry is considered to consist of a dominant fracture in the rock fabric. The scale of geometric irregularities along the surfaces of the fracture should be small when compared to the scale of the entire fracture surface. In contrast, a geometrically complex fracture system is made up of fractures and re-activated discontinuities of different sizes, shapes and orientations. A detailed definition on fracture geometry has been published by the ICR [4]

Fig. 7 Test-induced fracture shifted laterally when it met an elongated grain (muscovite), causing the crack to kink. Photomicrograph taken with a SEM.

The complexity in fracture geometry is largely controlled by the rocks' cementing materials and matrix, as well as by the spatial relationship between stress-induced fractures and fabric defects in the rocks. As demonstrated in Fig. 7, a propagating fracture was forced to shift laterally when it met the boundary of an elongated grain. The interactions between a propagating fracture and existing discontinuities or structural defects, as portrayed in Fig. 7, have important implications for the suddenness and rapidity of rock failures. Theoretical analyses [5] have shown that an array of structural defects ahead of a propagating fracture can significantly alter the fracture-tip stress field, causing either stress amplification or shielding. Either one of these two possible events dominates depending on the relative position, orientation and density of the defects in the zone around the fracture-tip. Intensified interactions between the stress-induced fractures and fabric elements of the rocks usually result in a complex fracture system, and consume more energy. Consequently, the resulting failure process is unlikely to be sudden and violent. In contrast, if a rock failure process is caused by the formation of one or a few dominant fractures, the potential energy in the 'roof–seam–floor' system, created by mining, can become excessive on

driving these fractures, and will render them highly unstable and violent, according to the conventional fracture mechanics principles [6].

Tests have been conducted on different rock types to study the suddenness of failure processes and their initiation in relation to the rocks' structural characteristics. In an extreme case, stress-induced fractures showed very limited interactions with the bulk of the rock fabric, observed during UCS tests of specimens from intrusive plutonic rock (diorite) samples containing healed and penetrative pre-existing fractures. The failure of the rock was significantly determined by the existing fractures. The surfaces of these pre-existing fractures are relatively planar, smooth and often coated. Importantly, a group of these fractures are oriented at approximately 20°–30° to the core axis, coinciding with the favourable spatial attitude for stress-induced fractures under UCS loading conditions.

Prior to testing, traces of the pre-existing fractures on the surfaces of intrusive rock test specimens were delineated by a coloured felt pen to assist with the identification of the response patterns of these structural defects to the applied forces.

The tests showed close correlations among UCS values, failure modes and the structural defects of the specimens. Specimens free of pre-existing fractures exhibited high UCS values, approximately 190 MPa on average, and they often developed significant spalling prior to failure as warning signals. The specimens shattered completely at failure.

Fig. 8. Different failure modes in specimens with and without pre-existing fracture planes.

In contrast, specimens with the favourably oriented pre-existing fractures failed, not only at much lower UCS values (averaging 62 MPa, with a minimum value of only 34 MPa), but also suddenly and without any warnings. The test-induced fractures were confined by the pre-existing fractures, as they followed exactly the geometry of existing fractures, and had very limited interactions with the bulk of the rock fabric.

Figure 8 is a photograph of the two distinctly different failure modes. The shattered fragments originated from a specimen with no traces of pre-existing fractures, whereas the other specimen shows a test-induced fracture following extremely closely an existing fracture, which is oriented at approximately 20°–30° to the core axis.

Test-induced fractures had demonstrable intensive interactions with the rock fabric, as observed in UCS tests, as well as in fracture toughness tests made on specimens of mudstones. The direction of loading (UCS tests) or fracture propagation (fracture tests) was normal to bedding in the specimens. Figures 9 and 10 show the fracture pattern in the brown mudstone specimens. The test-induced fractures were often arrested when they met bedding surface, and frequently forced to change orientation through the development of bed separation. As a consequence, these rock specimens developed a complex fracture network in UCS tests (Fig. 9) and irregular fracture surfaces in fracture tests (Fig. 10). The development of a complex fracture geometry, signifying an intensified interaction between the test-induced fractures and fabric elements, has resulted in a stable failure process of the rock specimens.

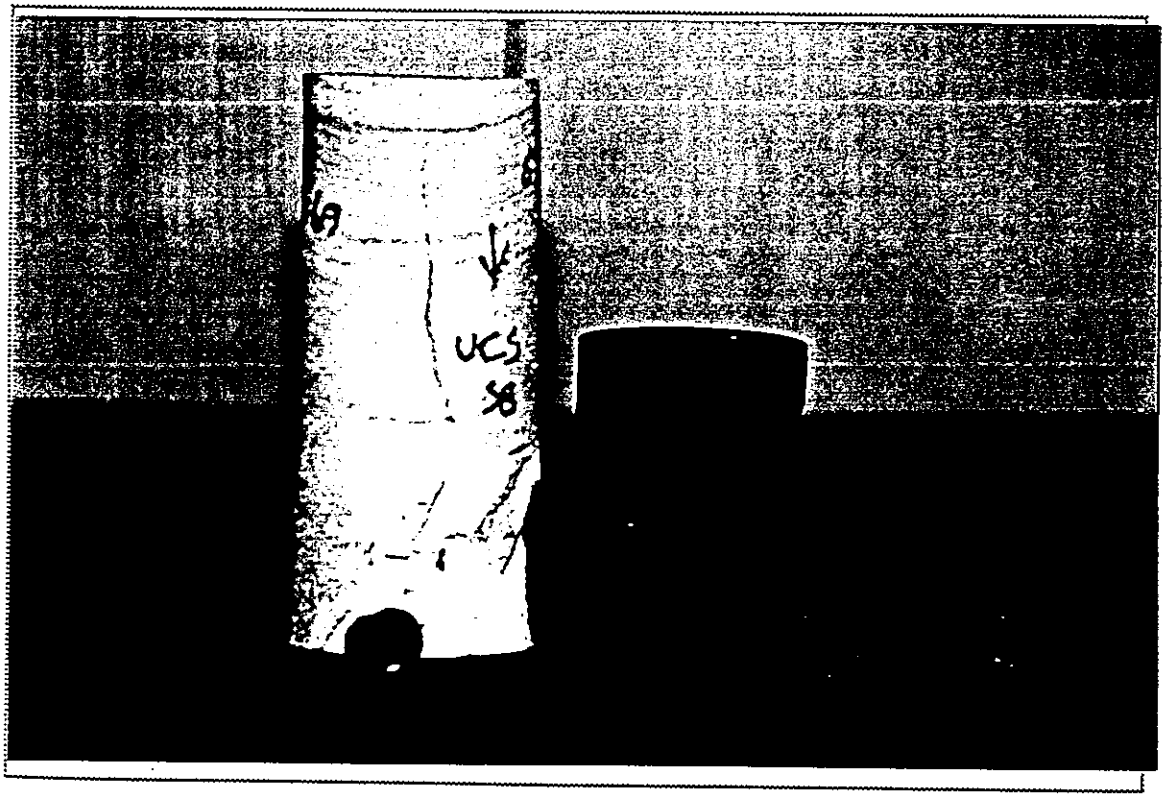

Fig. 9. Different fracture patterns developed in the specimens of lutateous rocks (brown colour) and sandstone (light grey colour)—UCS tests.

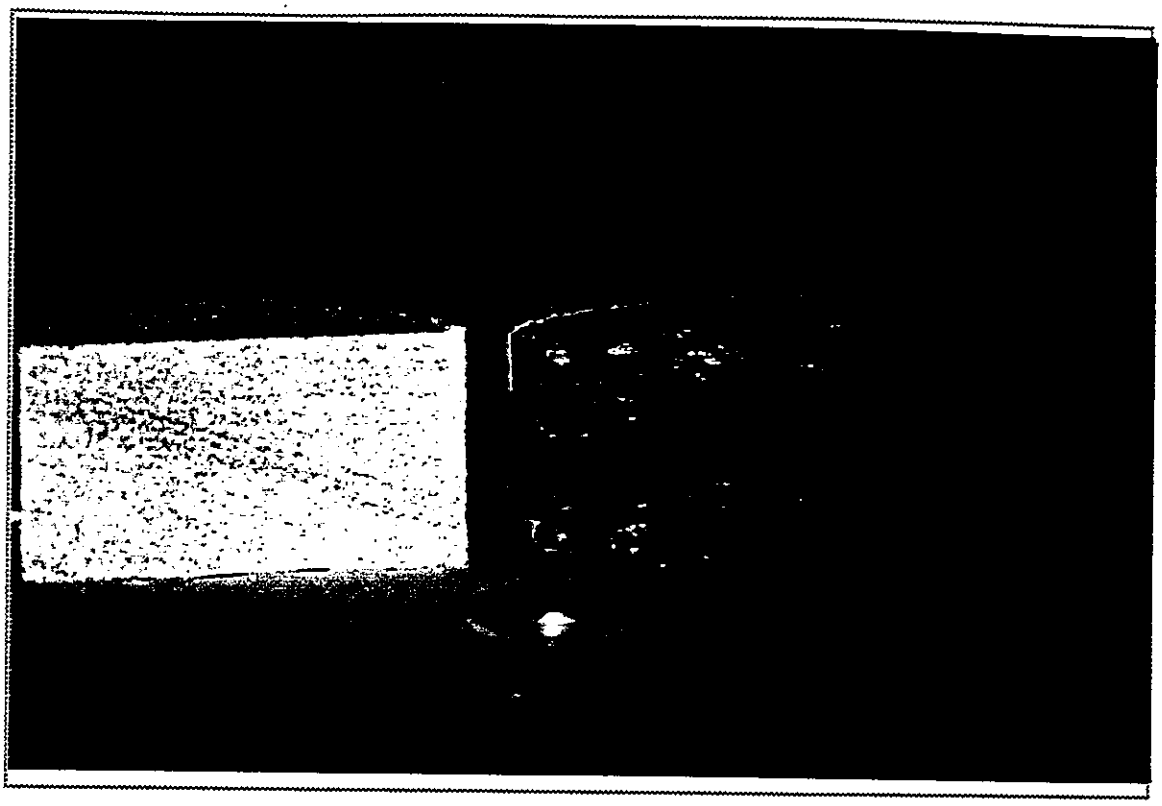

Fig. 10. Different fracture patterns developed in the specimens of mudstone (brown colour) and sandstone (light grey colour)—Fracture toughness tests.

Figures 9 and 10 also demonstrate the aspects of failed specimens of sandstone. The dominant and continuous fractures developed in UCS tests (Fig. 9), and the clearly defined and relatively smooth fracture surfaces generated in fracture toughness tests (Fig. 10), indicate that the interactions between fracturing and the bulk of the fabric of sandstone specimens were limited, in comparison with those in the mudstone and shale rocks.

Table 1
DATA SUMMARY FOR SANDSTONE SPECIMENS

DATA	MEAN	MINIMUM	MAXIMUM	RANGE	STD. DEV.	COUNT
UCS (Dry)	45.3	24.3	61.9	37.6	11.1	10
UCS (Wet)	29.3	17.4	49.5	32.1	9.2	8
Tensile Strength (Dry)	5.7	4.0	7.3	3.3	1.1	12
Tensile Strength (Wet)	2.7	2.0	3.4	1.4	.6	5
Fracture Toughness (Dry)	0.8	0.4	1.1	0.7	0.2	11
Fracture Toughness (Wet)	0.5	0.3	0.6	0.3	0.2	3

Unit: UCS: MPa
Tensile Strength: MPa
Fracture Toughness: $MPaM^{0.5}$

Std. Dev = Standard Deviation.

Table 2
DATA SUMMARY FOR MUDSTONE SPECIMENS (DRY)

DATA	MEAN	MINIMUM	MAXIMUM	RANGE	STD. DEV.	COUNT
UCS	30.4	15.9	52.5	36.6	11.2	11
Tensile Strength	2.0	0.9	3.8	2.8	0.9	12
Fracture Toughness	0.3	0.2	0.5	0.3	0.1	7

Unit: UCS: MPa
Tensile Strength: MPa
Fracture Toughness: $MPaM^{0.5}$
Std. Dev = Standard Deviation.

Tables 1 and 2 give summaries of data for the test specimens prepared from sandstone and mudstone, based on the original data given in Appendix A. Both rock types are moderately strong*, although there is a significant difference between the mechanical strength of the two rock types. The two rock types have distinctly different failure processes, reflecting the difference in interactions between fracturing and rock fabric, as discussed above. As shown in Figs 11 and 12, sandstone specimens, when subjected to uniaxial compressive loads, exhibit the typical 'Class II' failure behaviour [7]. In contrast, the mudstone specimens showed a 'Class I' failure pattern [7]. The 'Class II' failure behaviour was found in all tested sandstone specimens, irrespective of their moisture conditions. The different deformation characteristics, as indicated in Figs 11 and 12, indicate that under compressive loads, the tested sandstone specimens are more likely to fail violently and suddenly, even when wet, whereas the mudstone will fail gradually and progressively.

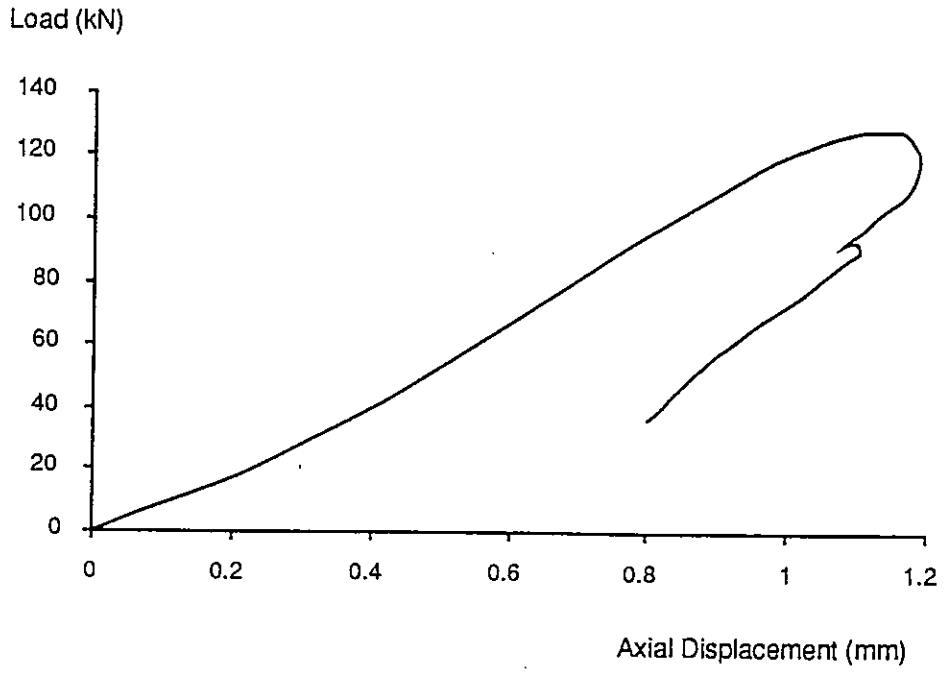

Fig. 11. Plot of load against axial displacement of a sandstone specimen showing Class II failure behaviour.

* The moderate strength category is for rocks with UCS values ranging from 25 to 50 MPa, according to the ISRM classification.

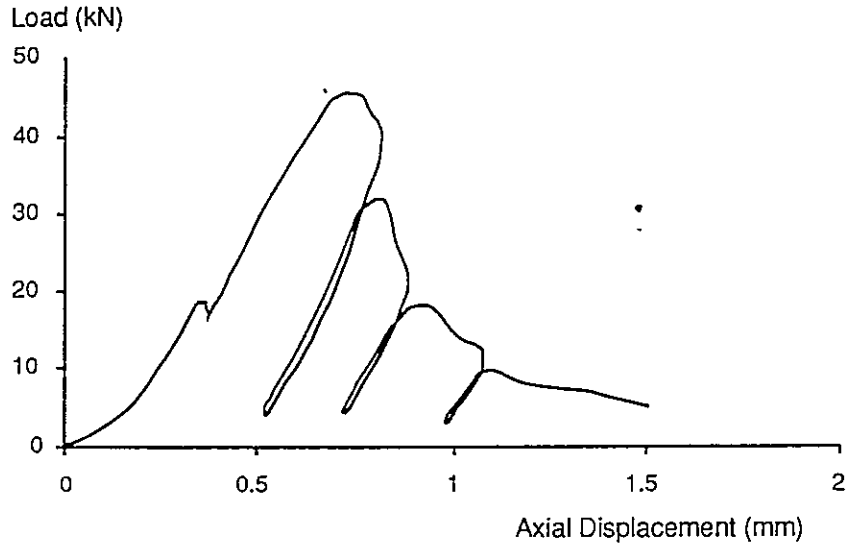

Fig. 12. Plot of load against axial displacement of a mudstone specimen showing Class I failure behaviour.

The tested sandstone and mudstone specimens described in this section of the report have been sampled in the overburden of the Bulli Seam, but not in the immediate roofstrata. The tests were done to establish test criteria for comparison of these well known rock types in the overburden of seams with the great variety of rock types in the immediate roofstrata.

VII. INTERPRETATION OF TEST RESULTS

The mechanical behaviour of strong rocks with fabric defects has demonstrated that fabric defects, joints, faults or erosional surfaces, contained in stronger rock units in the roof strata, require special attention, since rock failures caused by the re-activation of such defects, when favourably oriented in the stress field, can be violent and occur without warning.

It has been shown that coal measures rocks with clay mineral concentrations on the surfaces of well developed laminae, can offer moderately high fracture resistance when the mining induced fracture system develops normal, rather than parallel, to bedding. Importantly, the associated failure process will be stable with pre-failure fracture events as warning signals. However, fracture resistance of these rocks becomes very low, or even reaches zero, when fracturing takes place in the bedding planes when the failure process is likely to be rapid and sudden.

Mine openings normally have a rectangular profile that favours fracturing along bedding planes, due to gravity loading and shearing. Under such mining conditions, laminated roofstrata with bedding planes coated with clay minerals, will offer little resistance to fracturing, thus creating difficulties for strata control, particularly when these rocks are unsupported, as in highwall mining. For such difficult situations, the anisotropic fracture behaviour of the laminated rocks should be exploited by modifying the profile of the mine opening, so that the development of mining-induced fracture systems parallel to bedding is restrained. As a consequence, higher fracture resistance of the rock unit and stable failure processes may be achieved.

VIII. REFERENCES

[1] Ouchterlony, F., 1988. Suggested methods for determining the fracture toughness of rock. ISRM Commission on Testing Methods. Int. J. Rock Mech.Min.Sci. & Geomech. Abstr., 25: 71–96.

[2] Szendi-Horvath, G., 1980. Fracture toughness determination of brittle materials using small to extremely small specimens. Engng. Fract. Mech., 13: 955-961.

[3] Guo, H., Aziz, N.I. and Schmidt, L.C., 1993. Rock fracture toughness determination by Brazilian tests. Eng. Geology. 33: 177-188.

[4] Li, G., Moelle, K.H.R. and Sano, O., 1994. Rock fabrics and fracture propagation. *New Horizons in Resource Handling and Geo-Engineering*, Proceedings of 1994 MMIJ/AusIMM Joint Symposium, Japan, pp.477-484.

[5] Ortiz, M., 1987. A continuum theory of crack shielding in ceramics. J. Appl. Mech., 54: 54-58.

[6] Broek, D., 1982. Elementary Engineering Fracture Mechanics. Martinus Nijhoff Publishers, 469 pp.

[7] Brady B.H.G. and Brown E.T., 1993. Rock Mechanics for Underground Mining. Chapman & Hall, pp 571.

Appendix A

MECHANCIAL PROPERTIES OF ROCKS TESTED SINCE THE INSTALLATION OF THE MTS DEVICE

Specimen	Rock Type	Uniaxial Compressive Strength (MPa)	Uniaxial Tensile Strength (MPa)	Fracture Toughness ($MPaM^{0.5}$)
Cp 4	Shale	35.41		
Cp 5	Shale	30.33		0.63
Cp 6	Sandstone	45.35		0.78
Cp 7	Sandstone	47.39		0.71
Pk 1	Cindered coal	31.50		1.27
Pk 2	Cindered coal			1.41
Pk 3	Cindered coal	23.70		
Pk 4	Cindered coal	16.30		
Pk 5	Cindered coal	45.80		
Wy 1-1	Dolerite	91.23		
Wy 2-1	Dolerite	70.77		1.00
Wy 2-2	Dolerite	69.32		
Wy 3-1	Dolerite	33.97		0.86
Wy 4-1	Dolerite	40.89	9.27	1.14
Wy 4-2	Dolerite	54.50	10.71	1.06
Wy 4-3	Dolerite	44.78	7.21	
Wy 4-4	Dolerite	77.24	5.08	1.30
Wy 4-5	Dolerite	62.22	6.59	1.39
Wy 4-6	Dolerite	57.18	6.76	
Wy 4-7	Dolerite		5.99	
Sb 1-1	Siltstone	58.75		
Sb 1-2	Siltstone	61.52		1.39
Sb 1-3	Siltstone	38.25		
Sb 1-4	Siltstone	52.68		
Sb 1-5	Siltstone	39.71		
Sb 1-6	Siltstone	50.92		
Sb 1-7	Siltstone	66.18		
Sb 1-8	Siltstone	57.23		
Sb 2-1 (1)	Sandstone	78.83	6.52	1.26
Sb 2-1 (2)	Sandstone		7.19	
Sb 2-2 (1)	Sandstone	70.11	8.72	1.35
Sb 2-2 (2)	Sandstone		5.10	
Sb 2-3	Sandstone	75.80	8.15	1.20
Sb 2-4	Sandstone	80.42		1.21
Sb 2-5	Sandstone	76.44		
Sb 2-6	Sandstone	74.02		
Sb 3-0	Shale			
Sb 3-1	Shale	57.25		
Sb 3-2	Shale	60.92		
Sb 4-0	Shale			
Sb 5-1	Shale	36.50		

Appendix A (continued)

Specimen	Rock Type	Uniaxial Compressive Strength (MPa)	Uniaxial Tensile Strength (MPa)	Fracture Toughness ($MPaM^{0.5}$)
Sb 1-100	Siltstone		7.97	
Sb 1-101	Siltstone		7.11	
Sb 1-102	Siltstone		8.75	
Sb 3-100	Shale		9.14	
Sb 3-101	Shale		6.75	
Sb 3-102	Shale		9.36	
Sb 4-100	Shale		8.19	
Sb 5-100	Shale		6.27	
Sb 1 (1)	Sandstone		5.64	
Sb 1 (2)	Sandstone		3.15	
Sb C	Sandstone	17.40		0.67
Sb D	Sandstone		4.84	0.42
Sb E	Sandstone	24.30	3.96	0.49
Sb MV1	Shale		2.28	
Sb MV2	Shale	52.50		
Sb MV3	Shale			0.33
Sb N-1	Sandstone			0.22
Sb N-2 (1)	Sandstone		1.24	
Sb N-2 (2)	Sandstone	26.70	1.19	
Sb P1-1	Sandstone	15.90		0.18
Sb P1-2	Sandstone	23.90	1.07	
Sb P1-3 (1)	Sandstone		1.44	
Sb P1-3 (2)	Sandstone		1.24	
Sb P1-3 (3)	Sandstone		0.71	
Sb P1-3 (4)	Sandstone		0.90	0.05
Sb P2-1 (1)	Sandstone		2.23	
Sb P2-1 (2)	Sandstone		1.61	0.14
Sb P2-1 (3)	Sandstone		1.45	
Sb P2-2	Sandstone	9.80		
Sb P2-3 (1)	Sandstone			0.21
Sb P2-3 (2)	Sandstone			0.17
Sb P2-4	Sandstone	21.60		
Sb P2-5 (1)	Sandstone		1.48	0.10
Sb P2-5 (2)	Sandstone		1.35	
Sb WB22 68.4-68.8m	Sandstone	49.50		
Sb WB22 68.8-69.4m (1)	Sandstone	42.30	4.19	0.78
Sb WB22 68.8-69.4m (2)	Sandstone	28.10	3.40	
Sb WB22 68.8-69.4m (3)	Sandstone		4.78	
Sb WB22 69.4-70.0m (1)	Sandstone	57.70	5.31	0.78
Sb WB22 69.4-70.0m (2)	Sandstone		2.09	0.87
Sb WB22 70.1-70.4m (1)	Sandstone	61.90		
Sb WB22 70.1-70.4m (2)	Sandstone	27.30		
Sb WB22 72.2-72.4m (2)	Sandstone		6.90	0.90
Sb WB22 72.4-73.0m (1)	Sandstone	43.50	7.26	1.13
Sb WB22 72.4-73.0m (2)	Sandstone	32.60	2.80	
Sb WB22 73.0-73.4m	Sandstone	27.20		

Appendix A (continued)

Specimen	Rock Type	Uniaxial Compressive Strength (MPa)	Uniaxial Tensile Strength (MPa)	Fracture Toughness ($MPaM^{0.5}$)
Sb WB22 74.0-74.4m (1)	Sandstone	52.30	6.36	0.80
Sb WB22 74.0-74.4m (2)	Sandstone		3.03	
Sb WB22 74.6-74.9m (1)	Sandstone	51.90	6.26	
Sb WB22 74.6-74.9m (2)	Sandstone	27.40		
Sb WB22 75.6-76.0m	Sandstone	44.60	6.15	
Sb WB22 76.2-76.5m (1)	Sandstone		7.08	0.77
Sb WB22 76.2-76.5m (2)	Sandstone			0.48
Sb WB22 76.6-77.1m (1)	Sandstone	40.00		0.75
Sb WB22 76.6-77.1m (2)	Sandstone			0.59
Sb WB22 77.0-77.6m (1)	Sandstone	35.00	5.21	0.67
Sb WB22 77.0-77.6m (2)	Sandstone	24.60	2.04	
Sb WB23 150.20-150.30m	Shale	19.25		
Sb WB23 150.30-150.40m	Shale		2.88	
Sb WB23 150.48-150.58m	Shale	21.90		
Sb WB23 150.71-150.83m	Shale		0.96	
Sb WB23 150.88-150.97m	Shale		3.75	
Sb WB23 151.00-151.09m	Shale		1.33	
Sb WB23 152.30-152.40m	Shale	26.11		
Sb WB23 152.40-152.50m (1)	Shale			0.32
Sb WB23 152.40-152.50m (2)	Shale			0.37
Sb WB23 153.40.153.47m	Shale			0.29
Sb WB23 153.78-153.88m	Shale	15.90		
Sb WB23 154.00-154.10m	Shale		0.90	
Sb WB23 154.15-154.26m	Shale	22.77		
Sb WB23 154.26-154.41m	Shale	38.24		
Sb WB23 154.49-154.59m	Shale	25.65		
Sb WB23 154.74-154.86m	Shale	37.99		
Sb WB23 155.10-155.30m	Shale		1.74	
Sb WB23 155.30-155.40m	Shale		1.78	
Sb WB23 156.38-156.63m	Shale		2.97	
Sb WB23 155.40-155.54m	Shale	8.30		
Sb WB23 156.10-156.18m	Shale			0.54
Sb WB23 156.70-156.76m	Shale			0.32
Sb WB23 156.63-156.70m	Shale		1.48	
Sb WB23 157.10-157.20m	Shale	32.12		
Sb WB23 157.70-157.80m	Shale			0.24
Sb WB23 157.82-157.90m	Shale		2.12	
Sb WB23 158.10-158.23m	Shale		1.92	
Sb WB23 158.40-158.50m	Shale	42.45		
Sb 1530	Mudstone	28.64		
Sb 1531	Mudstone	28.02		
Sb 1532	Shale	62.00		
Sb 1533	Sandstone	65.20		
Sb 1534	Sandstone	49.12		
Sb 1535	Mudstone	33.23		
Sb 1536	Siltstone	43.93		

Appendix A (continued)

Specimen	Rock Type	Uniaxial Compressive Strength (MPa)	Uniaxial Tensile Strength (MPa)	Fracture Toughness ($MPaM^{0.5}$)
Sb 1537	Siltstone	68.04		
Sb 1538	Shale	31.91		
Sb 1539 (1)	Siltstone	39.56		
Sb 1539 (2)	Siltstone	50.62		
Mb 1	Coal	26.60		
Mb 3	Dolerite	99.60	11.43	
Mb 3-1 (1)	Dolerite		12.12	2.28
Mb 3-1 (2)	Dolerite		14.51	
Mb 3-1 (3)	Dolerite		14.03	
Mb 3-2 (1)	Dolerite		13.62	
Mb 3-2 (2)	Dolerite		12.66	
Mb 3-2 (3)	Dolerite		12.14	
Mb 3-3 (1)	Dolerite		13.47	2.51
Mb 3-3 (2)	Dolerite		15.37	
Mb 3-3 (3)	Dolerite		11.98	
Mb 4-1	Siltstone		1.99	
Mb 4-2	Siltstone		1.73	
Mb 4-3	Coal		3.76	
Mb 4-4	Coal		4.18	
Mb 4-5	Coal		4.15	
Mb 5	Shale		1.75	
Mb 5-0	Coal	25.50		
Mb 5-1	Coal		6.15	0.33
Mb 5-2	Coal		4.01	0.23
Mb 5-3	Coal		3.88	0.24
Mb 5-4	Coal			0.31
Mb 5-5	Coal		3.15	0.24
Mb 6-1	Dolerite	92.78	9.46	1.00
Mb 6-2	Dolerite	81.08	7.84	1.57
Mb 6-3	Dolerite	83.75	10.99	1.58
Mb 6-4	Dolerite	111.85	14.57	2.07
Mb 6-5	Dolerite	73.63	3.90	1.53
Mb 7 (1)	Shale		2.04	
Mb 7 (2)	Shale			
Mb 8 (1)	Shale		2.81	
Mb 8-1	Cindered coal		5.65	0.60
Mb 8-2	Cindered coal		3.28	
Mb 8-3	Cindered coal		8.91	
Mb 8-4	Shale		5.13	
Mb 8-2 (1)	Cindered coal		2.42	0.22
Mb 8-2 (2)	Cindered coal		3.42	
Mb 8-5	Cindered coal	21.94		0.55
Mb 8-6	Cindered coal	30.15		
Mb DDH 450 129.90-130.19m (1)	Siltstone			0.49
Mb DDH 450 129.90-130.19m (2)	Siltstone			0.31
Mb DDH 450 133.33-134.07m	Cindered coal		9.10	2.18

Appendix A (continued)

Specimen	Rock Type	Uniaxial Compressive Strength (MPa)	Uniaxial Tensile Strength (MPa)	Fracture Toughness ($MPaM^{0.5}$)
Mb DDH 450 135.26-135.43m	Cindered coal	72.80		
Mb DDH 450 137.40-137.70m	Cindered coal			0.93
Mb DDH 467 139.00-139.18m	Siltstone		4.18	
Mb DDH 467 134.17-134.66m (1)	Dolerite		10.14	
Mb DDH 467 134.17-134.66m (2)	Cindered coal	56.60	6.79	
Mb DDH 467 134.17-134.66m (3)	Dolerite		7.94	1.52
Mb DDH 467 134.17-134.66m (4)	Dolerite		7.23	
Mb DDH 467 132.14-132.48m (1)	Dolerite		11.05	1.84
Mb DDH 467 132.14-132.48m (2)	Dolerite		15.76	
Mb DDH 467 131.48-131.85m (1)	Cindered coal		7.06	
Mb DDH 467 131.48-131.85m (2)	Cindered coal		5.94	
Mb DDH 467 131.48-131.85m (3)	Cindered coal		7.39	
Mb DDH 467 129.36-129.58m (1)	Siltstone			0.42
Mb DDH 467 129.36-129.58m (2)	Siltstone			0.33
Mb DDH 462 128.38-128.76m (1)	Cindered coal		5.89	1.25
Mb DDH 462 128.38-128.76m (2)	Cindered coal			0.99
Mb DDH 462 122.33-122.68m	Shale	55.20	10.45	0.57
Mb DDH 462 125.00-125.22m	Dolerite			1.75
Mb DDH 467 129.00-129.19m	Shale		5.74	
Mb 1B	Coal		2.87	0.21
Mb 1C	Coal		3.83	
Mb 1A	Coal		2.36	
Mb 5A	Coal		3.91	0.23
Mb 1D	Coal	33.20		
Gretley1	Siltstone	59.36	6.97	
Gretley2	Siltstone	71.87		
Gretley3	Siltstone	49.56		
Gretley4	Siltstone	67.23		
Gretley5	Siltstone	55.65		
El A	Conglomerate	50.80		
El B	Sandstone	34.06		
El C	Sandstone	46.74		
El D	Sandstone	52.03		
El E	Conglomerate	84.73		
El F	Sandstone	71.17		
Cum 1	Mudstone	6.11		
Cum 2	Mudstone	0.46		
Cum 3	Mudstone	9.12		
Cum 4	Mudstone	14.51		
Cum 5	Mudstone	20.40		
Cum L-1	Mudstone	8.06		
Cum L-2	Mudstone	19.28		
Cum L-3	Mudstone	17.06		
Cum L-4	Mudstone	1.53		
Cum L-5	Mudstone	8.33		
Cum S-1	Mudstone	10.35		

Appendix A (continued)

Specimen	Rock Type	Uniaxial Compressive Strength (MPa)	Uniaxial Tensile Strength (MPa)	Fracture Toughness ($MPaM^{0.5}$)
Cum S-2	Mudstone	18.40		
Cum S-3	Mudstone	29.23		
Cum S-4	Mudstone	16.09		
Cum S-5	Mudstone	13.93		
Cum S-6	Mudstone	11.83		
Hp A-1	Coal	41.77		
Hp A-2	Coal	46.61		
Hp W-1	Coal	4.20		
Pa S1 (1)	Coal			0.13
Pa S1 (2)	Coal			0.17
Pa S1 (3)	Coal			0.19
Pa S2 (1)	Coal			0.26
Pa S2 (2)	Coal			0.21
Pa S2 (3)	Coal			0.17
Pa S2 (4)	Coal			0.22
Op 6-3	Diorite	56.34		1.34
Op 6-4	Diorite	186.26		1.38
Op 6-6	Diorite	94.73		1.89
Op 6-7	Diorite	67.09	11.80	
Op 6-9	Diorite	58.52		1.90
Op 7-1	Diorite	104.75		
Op 7- 3	Diorite	34.29		1.91
Op 7-4	Diorite	193.86		1.51
Op 7-5	Diorite	182.20		1.52
Op 7-7	Diorite	115.49		1.56
Op 7-9	Diorite	48.85		1.97
Op GRS 15	Diorite	75.29		
Op GRS 101	Diorite	63.08		
Op GRS 37-221	Diorite			1.43

Appendix B

MECHANICAL DATA FOR LAMINATED ROCKS FROM IMMEDIATE ROOF AND FLOOR STRATA

The rock types tested include mudstone, siltstone, shale and sandstone

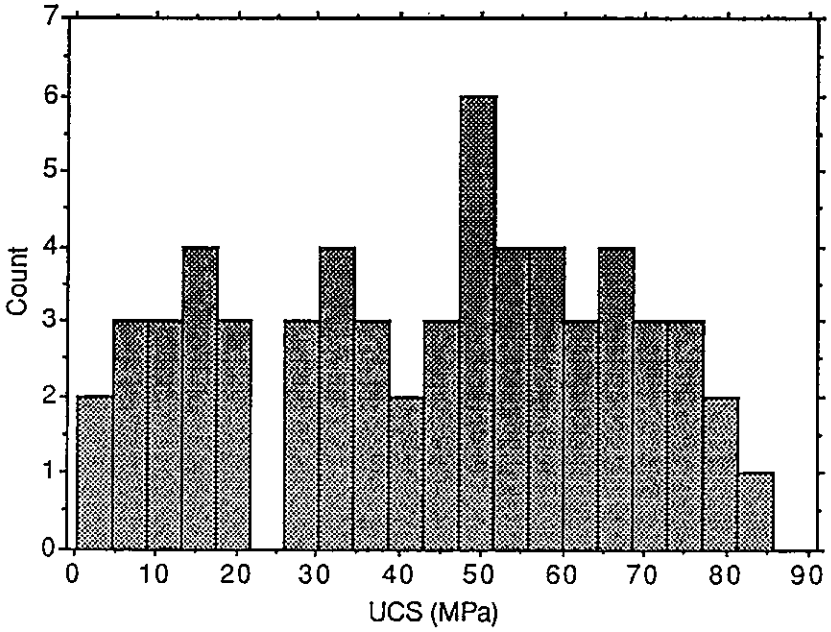

A. Frequency Distribution of Uniaxial Compressive Strength Data (UCS)

DATA SUMMARY OF UCS TESTS

Mean	Std. Dev.	Minimum	Maximum	Range	No. Tests
43.3 MPa	23.1 MPa	0.5 MPa	84.7 MPa	84.3 MPa	60

Two observations can be made on the results displayed in Figures A and B:

(1) The strength values vary widely due to the different lithologies of the tested rocks. Laminated sandstones generally show high strength, especially those with siliceous and carbonate cement. Mine design must make provision for this wide range of values.

(2) 25% of the rock samples tested show very low strength (UCS <11 MPa). Loading direction is normal to bedding for these very weak rocks. The strength values of these rocks will be extremely low when bed separation is the main failure rate.

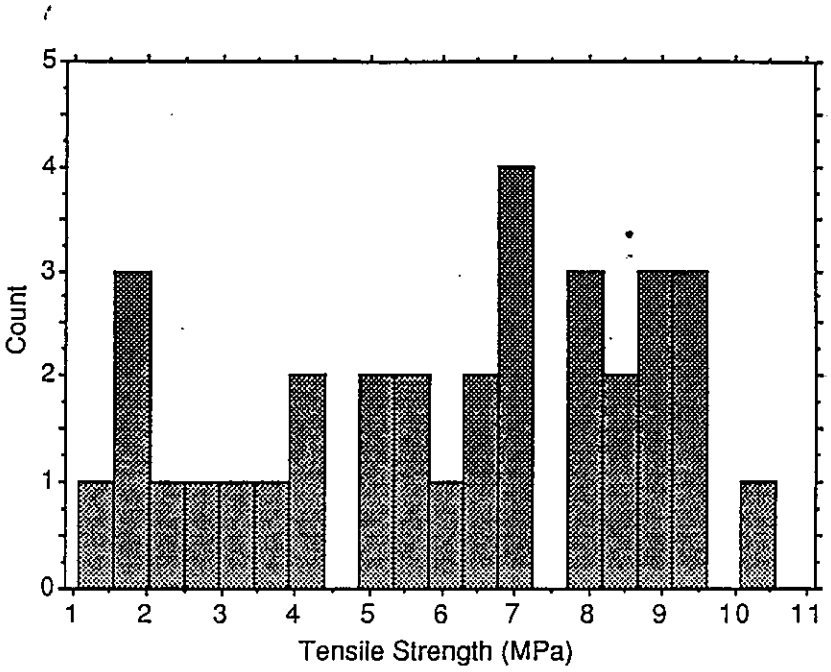

B. Frequency Distribution of Uniaxial Tensile Strength Data Obtained by Brazil Tests

DATA SUMMARY OF BRAZIL TESTS

Mean	Std. Dev.	Minimum	Maximum	Range	No. Tests
6.1 MPa	2.7 MPa	1.1 MPa	10.4 MPa	9.4 MPa	33